Free Radical Biology and Medicine 141 (2019) 383–392

Contents lists available at ScienceDirect

Free Radical Biology and Medicine

journal homepage: www.elsevier.com/locate/freeradbiomed

miR-15b induces premature ovarian failure in mice via inhibition of α-Klotho expression in ovarian granulosa cells

Te Liu[a,*], Yan Liu[b], Yongyi Huang[c], Jiulin Chen[a], Zhihua Yu[a], Chuan Chen[a,**], Lingyun Lai[d,***]

[a] Shanghai Geriatric Institute of Chinese Medicine, Shanghai University of Traditional Chinese Medicine, Shanghai, 200031, China
[b] Department of Ophthalmology, Shanghai General Hospital, Shanghai Jiao Tong University School of Medicine, Shanghai, 200080, China
[c] Shanghai Topbiox Co. Ltd, Shanghai, 200031, China
[d] Department of Nephrology, Huashan Hospital, Fudan University, Shanghai, 200040, China

ARTICLE INFO

Keywords:
Premature ovarian failure
Ovarian granulosa cells
α-Klotho
microRNA
Autophagy
Oxidative stress

ABSTRACT

A thorough understanding of epigenetics regulatory mechanisms of premature ovarian failure (POF) is still lacking. Here, we found that cyclophosphamide induced significantly decrease in α-Klotho (*Kl*) expression in mouse ovarian granulosa cells (mOGCs), suggesting that cyclophosphamide inhibited *Kl* expression. Cyclophosphamide also significantly accelerated ageing and led to a decline in the pregnancy rate of *C. elegans*. We subsequently noted that the pathological condition exhibited by $Kl^{-/-}$ mice was similar to that observed in cyclophosphamide-induced POF mice. Furthermore, the mOGCs in both types of mice showed significant signs of oxidative stress damage, including decreased SOD and ATP, increased ROS levels. Detailed analyses revealed that the decreased *Kl* expression led to the reduced expression of autophagy-related proteins in mOGCs, which resulted in decreased autophagy activity. Finally, we found that cyclophosphamide attenuated the autophagy function of mOGCs via upregulating microRNA-15b expression, which silenced the endogenous *Kl* mRNA expression and stimulated the activity of the downstream TGFβ1/Smad pathway. Therefore, we demonstrated that *Kl* was one of the key inhibitory factors in the development of POF. It elucidated the underlying epigenetic regulatory mechanism, whereby cyclophosphamide-dependent microRNA-15b inhibited *Kl* expression, leading to the reduced ability of mOGCs to induce autophagy and ROS scavenging, ultimately causing POF.

1. Introduction

Premature ovarian failure (POF) refers to the development of amenorrhoea before the age of 40 due to a failure in ovarian function [1–7]. It is characterised by primary or secondary amenorrhoea with elevated gonadotropin levels and reduced oestrogen levels in the blood, accompanied by follicular atresia and a persistent reduction in the follicular reserve capacity [8–12]. POF has a significant impact on the quality of pregnancy in women, and there are currently no effective treatment measures or therapeutic drugs available [1–4,8–11]. Our previous studies have found that pathological aging of ovarian granulosa cells can significantly lead to POF [11,13]. And, we reported that induction of miR-15a expression by tripterygium glycosides caused mice POF by suppressing the Hippo-YAP/TAZ signalling effector Lats1 [13]. These information suggest that microRNA plays an important role in regulating the pathogenesis of ovarian pathological aging, but the in-depth mechanism is not clear.

Klotho (α-Klotho, *Kl*) was originally identified as an ageing-suppressor gene that was predominantly expressed in the kidneys and choroid plexus [14–20]. The human *Kl* gene encodes the α-Klotho protein, which is a multifunctional protein that regulates the metabolism of phosphate, calcium, and vitamin D, and it can also function as a hormone [17,21–26]. The proteins encoded by the *Kl* gene exist in three forms: full-length transmembrane KL, truncated soluble KL, and secreted Klotho (sKL). Soluble KL is generated via the release of the extracellular domain of the transmembrane protein, whereas sKL can be generated via alternative RNA splicing [15–17,27]. In mice, the overexpression of *Kl* products prolongs their lifespan [14,16,22–26,28], whereas knockout of the *Kl* gene accelerates ageing and shortens their lifespan [14,16,22–26,28]. And, sKL decreases with age in mice and humans, and can suppress the transforming growth factor beta 1 (TGF-β1)-induced Wnt/β-catenin signalling and the insulin-like growth factor

* Corresponding author.
** Corresponding author.
*** Corresponding author.
E-mail addresses: liute1979@126.com (T. Liu), ch9453@126.com (C. Chen), lylai89@163.com (L. Lai).

https://doi.org/10.1016/j.freeradbiomed.2019.07.010
Received 26 March 2019; Received in revised form 10 June 2019; Accepted 12 July 2019
Available online 13 July 2019
0891-5849/

List of abbreviations

3′UTR	3′Untranslated region
AKI	Acute kidney injury
AMH	*Anti*-Mullerian hormone
ATP	Adenosine triphosphate
bFGF	basic fibroblast growth factor
C. elegans	*Caenorhabditis elegans*
CKD	Chronic kidney disease
CTX	cyclophosphamide
DMEM:F12	Eagle Medium: Ham's F-12 medium
E2	Estradiol
EGF	Epidermal growth factor
FBS	Foetal bovine serum
FSH	Follicle-stimulating hormone
Gh	Growth hormone
IGF	Insulin-like growth factor
IIS	insulin/insulin-like growth factor-like signalling
Kl	Klotho
mOGCs	Mouse ovarian granulosa cells
NGM	Nematode growth media
PBS	Phosphate-buffered saline
POF	Premature ovarian failure
ROS	Reactive oxygen species
sKL	secreted Klotho
SOD	Superoxide dismutase
TGF-β1	Transforming growth factor beta 1
WT	Wild-type

1 (IGF-1)-induced fibrosis and signal transduction pathways [14,16,17,23–26,29]. *Kl*$^{-/-}$ mice exhibit growth retardation, osteoporosis, ectopic calcification in soft tissue, early onset of tissue ageing, and mortality at nine weeks [14,16,17,23–26,29]. In addition, *Kl*$^{-/-}$ mice display severe skeletal muscle atrophy and an activated autophagy-lysosome pathway. The signal transduction activity of the autophagy inhibitor mTOR is suppressed, which is thought to be due to the lack of essential amino acids in the *Kl*-deficient glomeruli. In *Kl*$^{-/-}$ mice, there is a decrease in LC3 expression, and autophagy is significantly reduced. This phenomenon occurs concurrently in the brain tissues and skeletal muscles of the *Kl*$^{-/-}$ mice [29]. With regard to the maintenance of stem cell characteristics, a study has reported that the proliferation and differentiation of adipose-derived stem cells in *Kl*$^{-/-}$ mice are significantly reduced. Further investigations reveal that KL suppresses TGF-β1 and promotes peroxisome proliferator-activated receptor gamma (*PPAR-gamma*) expression and lipid formation, whereas the loss of KL leads to the overexpression of TGF-β1 and its downstream molecule Smad2/3 in the adipose-derived stem cells, resulting in cellular fibrosis and the progressive loss of the original stemness [30].

POF becomes phenotypically obvious, being detectableat 8 weeks of age in female *Kl*$^{-/-}$ mice. However, the relationship between the occurrence of this pathological condition and KL has not been elucidated. In this study, we investigated the role and effect of KL on maintaining the activity of mOGCs through the study of oxidative stress and autophagy. Meanwhile, we unexpectedly discovered that the *Kl* gene was one of the potential targets of miR-15b, thereby demonstrating the negative regulatory effect of miR-15b overexpression on the activity of mOGCs.

2. Materials and methods

A detailed description of all materials and methods can be found in Supplement SM.

2.1. Transgenic mice and Caenorhabditis elegans

Genetic αKlotho hypomorphic female mice with α-Klotho homozygous deficiency (kl$^{-/-}$) were previously described [14,31]. All female mice and N2 wild type (WT) *Caenorhabditis elegans* (*C. elegans*) were purchased from Modelorg (Shanghai Model Organisms Company, Shanghai, China).

2.2. microRNA purification and quantitation analysis

The microRNA was extracted from the cells in each group according to the manual of the miRcute miRNA Isolation Kit (TIANGEN Biotech (Beijing)Co.,Ltd., China). After microRNA was treated with Dnase I (Sigma-Aldrich, St. Louis, USA), it was quantified and reverse transcribed to synthesize cDNA using a miRcute miRNA First-strand cDNA (TIANGEN Biotech (Beijing)Co.,Ltd., China). Quantitative reverse transcription polymerase chain reaction (qPCR) was completed with RealPlex4 real-time PCR detection system (Eppendorf Co., Ltd., Hamburg, Germany), and miRcute miRNA qPCR Detection (TIANGEN Biotech (Beijing)Co.,Ltd., China) was used as the fluorescent dye for microRNA amplification. The qPCR process included a total of 40 amplification cycles: first, 94 °C denaturation for 120 s. Then, 94 °C denaturation for 20 s; 60 °C annealing for 34 s. The $2^{-\Delta\Delta Ct}$ calculation method was used to determine the relative gene expression level, where $\Delta Ct = Ct\_microRNA - Ct\_18S\ rRNA$; $\Delta\Delta Ct = \Delta Ct\_all\_groups - \Delta Ct\_control\_group$. The microRNA expression level was normalized to the expression level of 18S rRNA. The primers were in Table S1.

2.3. The mouse model of POF

The study protocol was in accordance with the article [3,11,13]. 10-week-old hebetic female C57BL/6 mice (n = 24) were randomized into two groups (POF group and WT group), with 12 mice in each group. POF mice were first injected intraperitoneally with cyclophosphamide at 70 mg/kg (Sigma-Aldrich, St Louis, USA), followed by intraperitoneal injection of cyclophosphamide at 30 mg/kg once every 2 days for 2 consecutive weeks, to construct the POF mouse model. In addition, the control group mice were injected intraperitoneally with the same amount of normal saline once every 2 days for 3 consecutive weeks. The study was approved by the Ethics Committee at the Shanghai Institute of Geriatrics (SHAGESYDW2018010). All experiments are in line with China National Science and Technology Commission animal laboratory regulations.

2.4. Isolation and culture of mouse ovarian granulosa cells (mOGCs)

According previous study [3,11,13], briefly, seven-week-old female C57BL/6 mice were purchased from the Experimental Animal Centre of Shanghai University of Traditional Chinese Medicine. The mice were sacrificed by cervical dislocation. Ovarian tissues were isolated under sterile conditions and were placed in 4 °C phosphate-buffered saline (PBS). The ovarian tissues were minced, and 2.0 ml of hyaluronidase (0.1%, Sigma-Aldrich, St. Louis, MO, USA) was added to the tissues for 1 min of digestion at 37 °C. The tissue suspension was gently pipetted, and 200 μl of foetal calf serum (Gibco, Gaithersburg, MD, USA) was added to the suspension to terminate the digestion; the suspension was then filtered by a 200-mesh cell strainer. Next, 5.0 ml of PBS was added to the filtrate and mixed well, followed by centrifugation at 1500 r/min for 5 min at 10 °C. The supernatant was discarded, and the pellet was re-suspended in 5.0 ml of PBS, followed by centrifugation at 1500 r/min for 5 min at 10 °C. The supernatant was discarded, and the cell pellet was re-suspended with Dulbecco's Modified Eagle Medium: Ham's F-12 medium (DMEM:F12) (1:1) and mixed well; the medium contained 10% foetal bovine serum, 10 ng/ml basic fibroblast growth factor (bFGF),

10 ng/ml epidermal growth factor (EGF), 2mML-glutamine, 10 ng/ml growth hormone (Gh), and 15 ng/ml estradiol (E2) (Gibco, Gaithersburg, MD, USA). The cell suspension was seeded in 6-well cell culture plates, which were then incubated at 37 °C with 5% CO2 until 80% confluency.

2.5. Behavioural and fertility measurements in C. elegans

Approximately 40 *Caenorhabditis elegans* (*C. elegans*) in the L4 larval stage were collected for each group. The *C. elegans* nematodes were individually picked and placed onto a nematode growth media (NGM) plate seeded with *Escherichia coli* OP50 and observed under the microscope. The number of head thrashes and body bends per minute were counted, and the frequency was calculated.

*C. elegans*in the L4 larval stage were randomly picked and placed onto the NGM plates of the experimental and control groups. One *C. elegans* was placed on each medium plate and maintained at 20 °C. Once every 12 h, a single *C. elegans* nematode was removed and placed onto a freshly prepared NGM plate containing CTX, until the reproductive period ceased. The number of progeny on each NGM plate was then counted.

2.6. Statistical analysis

Each experiment was performed as least thrice, and data were shown as the mean - standard error where applicable; differences were evaluated with Student's *t*-test. A *p* value less than 0.05 was considered statistically significant.

3. Results

CTX damaged the ovary and shortened the lifespan of *C. elegans* through suppressing the expression of endogenous α-Klotho.

A mouse model of POF was established via intraperitoneal injection of CTX. Pathological examination revealed that mature follicles disappeared in the ovarian tissue of the POF mice, and there was an increased number of atretic follicles. The weight of the ovary was significantly reduced, and the cell quality of mOGCs was decreased (Fig. 1A, B, 1C). Immunofluorescence staining showed that wild-type (WT) mOGCs (*Anti*-Mullerian hormone [AMH+]) exhibited high expression of the α-Klotho protein, whereas α-Klotho expression was significantly reduced in POF mOGCs (Fig. 1D). Meanwhile, the qPCR and Western blot results demonstrated that both mRNA and protein levels of α-Klotho in POF mOGCs were significantly lower than that in the WT group (Fig. 1E and F, Supplement Data Fig. S2). In addition, the estradiol (E2) concentration in the peripheral blood of mice in the POF group was also considerably lower than that in the WT group (Fig. 1G). These results suggested that the expression of α-Klotho was significantly reduced in mOGCs of the POF mice.

Additionally, we selected *C. elegans* as another biological model to validate our hypothesis in a different organism, and investigated the effects of CTX on their behaviour and lifespan. The results from the experiments showed that the lifespan of *C. elegans* in the CTX-treated group was significantly shortened (Fig. 2A). The frequencies of head thrashes and body bends were considerably lower compared with the control group (PBS-treated group) (Fig. 2B and C, Supplement Video CTX, Supplement Video PBS). The number of progenywas also significantly lower in *C. elegans* of the CTX group compared with the control group (Fig. 2D). Meanwhile, the percentage of *C. elegans* positive for lipofuscin was significantly higher in the CTX group compared with the control group (Fig. 2E). It has been reported that *C. elegans* harbours two ceKlotho genes that are homologous to the mammalian Klotho gene: C50F7.10 and E02H9.5 [32–36]. The lifespan of *C. elegans* is co-regulated by the insulin/insulin-like growth factor (IGF)-like signalling (IIS) pathway and ceKlotho. We analysed the expression of the related genes in each group of *C. elegans* using qPCR. The results showed that the expression level of the ceKlotho gene C50F7.10 was significantly lower in the CTX group, whereas the expression of E02H9.5 was not noticeably different from the control (Fig. 2F). The expression levels of the key factors of the IIS pathway EGL-17, EGL-15,

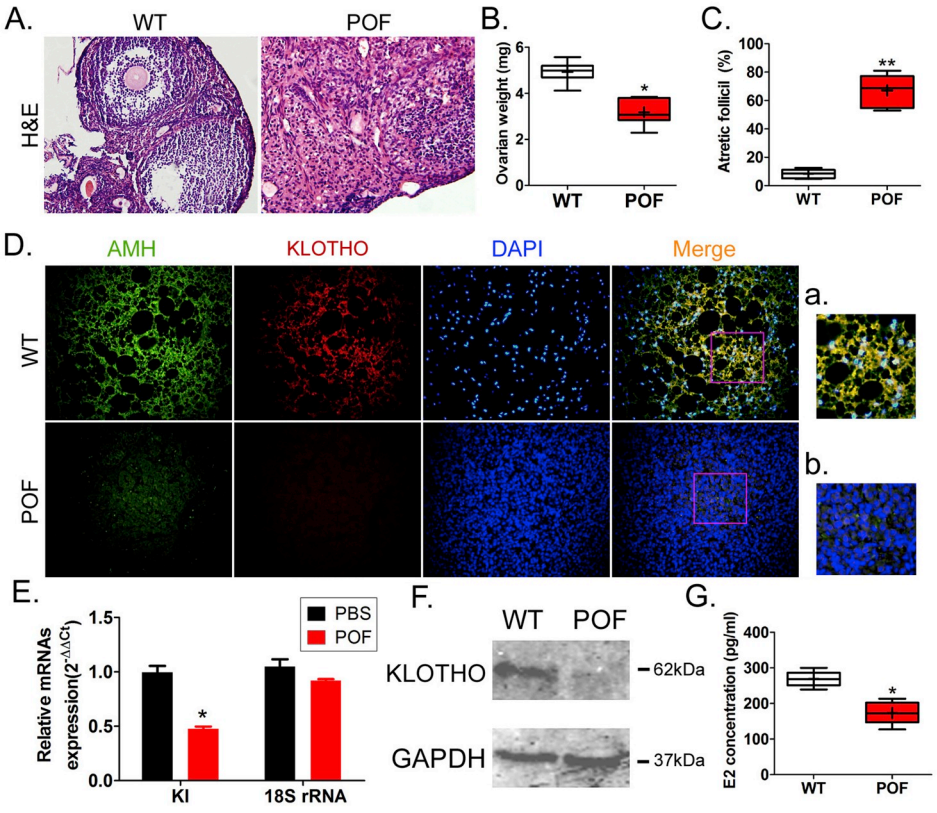

Fig. 1. CTX induces POF in mice and down-regulates Klotho expression in mouse ovarian tissue. (A) Hematoxylin-eosin (H&E) staining of mouse ovarian tissue. Magnification, 200 × . (B) Measurement of ovary weights in each group of mice. *p < 0.05 vs WT group; *t*-test; n = 6. (C) Determination of the proportion of atretic follicles in each group of mice. **p < 0.01 vs WT group; *t*-test; n = 6. (D) Immunofluorescence staining showing the expression levels of Klotho protein in the mOGCs (AMH+) in each group. Magnification, 200 × . The a and b are high power views of pink square boxes. Magnification, 400 × . (E) qPCR showing the expression levels of *Kl* mRNA in the ovarian tissues of each group of mice. *p < 0.05 vs PBS group; *t*-test; n = 6. (F) Western blot showing the expression levels of Klotho protein in the ovarian tissues of each group of mice. (G) Enzyme-linked immunosorbent assay (ELISA) showing the E2 concentration in the peripheral blood of mice in each group. *p < 0.05 vs PBS group; *t*-test; n = 6. (For interpretation of the references to colour in this figure legend, the reader is referred to the Web version of this article.)

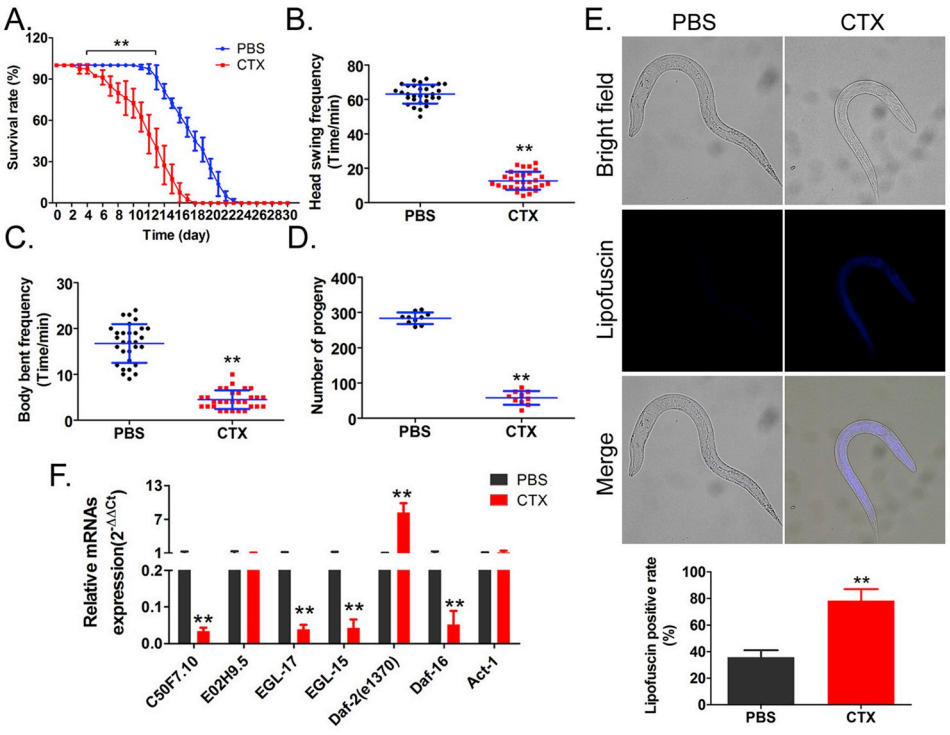

Fig. 2. CTX shortens the lifespan of *C. elegans* and inhibits ceKlotho and the activity of theIIS signalling pathway. (A) CTX significantly shortens the lifespan of *C. elegans*. **p < 0.01 vs PBS group; *t*-test; n = 40. (B) CTX significantly reduces the head swing frequency of *C. elegans*. **p < 0.01 vs PBS group; *t*-test; n = 40. (C) CTX significantly reduces the body bend frequency of *C. elegans*. **p < 0.01 vs PBS group; *t*-test; n = 40. (D) CTX significantly reduces the reproductive capacity of *C. elegans*. **p < 0.01 vs PBS group; *t*-test; n = 40. (E) CTX significantly promotes the deposition of lipofuscin in *C. elegans*. **p < 0.01 vs PBS group; *t*-test; n = 40. (F) qPCR showing the mRNA expression levels of ceKlotho and the key factors of the IIS signalling pathways in each group of *C. elegans*. **p < 0.01 vs PBS group; *t*-test; n = 3.

and Daf-16 were significantly reduced in *C. elegans* in the CTX group, whereas the expression level of Daf-2 was significantly elevated (Fig. 2). These results showed that CTX could shorten the lifespan of *C. elegans* and inhibit their reproductive ability by suppressing the activation of ceKlotho and the IIS pathway in *C. elegans* [32–36]. Therefore, CTX acts through suppression of Klotho and the IGF-like signalling pathway in *C. elegans*.

Supplementary video related to this article can be found at https://doi.org/10.1016/j.freeradbiomed.2019.07.010.

3.1. $Kl^{-/-}$ mice exhibited a POF phenotype with a significantly reduced level of autophagy in mOGCs

We examined the ovarian tissues of mice with homozygous deletion of *Kl* ($Kl^{-/-}$) using pathological and biochemical methods. The results showed that mature follicles were almost completely lost in the ovarian tissues of $Kl^{-/-}$ mice, and the number of atretic follicles was significantly increased (Fig. 3A and C). There was also a considerable reduction in the weight of the ovary (Fig. 3B). Moreover, the concentration of E2 in the peripheral blood was significantly lower than in WT mice, whereas the concentration of follicle-stimulating hormone (FSH) was higher (Fig. 3D). These ovarian ageing phenomena are very similar to the pathological features displayed by mice with CTX-induced POF. Besides, Western blot analysis showed that the expression of AMH and α-Klotho in the ovarian tissue of $Kl^{-/-}$ mice was considerably lower than that of WT mice (Fig. 3E, Supplement Data Fig. S2). And, the expression of the autophagy-related proteins Beclin 1 and LC3I/II was also significantly reduced, whereas the expression of the autophagy-inhibitory protein p62 was increased (Fig. 3E, Supplement Data Fig. S2). The results of immunofluorescence staining were in line with those of the Western blot, which showed that the signal for α-Klotho protein expression was low in mOGCs, and the signals for autophagy-related proteins were also extremely low (Fig. 3F, Supplement Data Fig. S1). Meanwhile, transmission electron microscopy showed that in the mOGCs of the ovarian tissue of $Kl^{-/-}$ mice, there was a significant reduction in the number of mitochondria, poorer structural integrity, and a significant decrease in the number of autophagosomes (Supplement Data Fig. S3). So, we also found that the level of autophagy in the mOGCs of $Kl^{-/-}$ mice was significantly reduced. These results suggested that $Kl^{-/-}$ mice exhibited POF, and the level of autophagy in mOGCs was significantly reduced.

3.2. mOGCs in POF mice had significantly reduced ability in both ROS scavenging and ATP synthesis

The results of the ROS assay showed that the ROS levels in the mOGCs of both the CTX-induced POF mice and $Kl^{-/-}$ mice were noticeably higher than those in the WT mice (Fig. 4A). Above result suggested that the mOGCs from CTX-induced POF mice and Kl−/− mice had reduced ability in ROS scavenging. However, the SOD levels in mOGCs were significantly lower in the CTX (POF) and $Kl^{-/-}$ mice than in the WT mice (Fig. 4B). Meanwhile, the ATP levels in the mOGCs of the CTX (POF) and $Kl^{-/-}$ mice were also significantly lower than those in the WT mice (Fig. 4C). These results suggested that the mOGCs in POF mice had reduced ability in both ROS scavenging and ATP synthesis, which was likely associated with the loss of mitochondria and the reduced capacity for autophagy.

3.3. miR-15b induced mOGCs apoptosis via the targeted suppression of KL expression

To elucidate the mechanism by which the CTX-induced downregulation of α-Klotho expression led to POF, we analysed the expression status of the potential microRNAs that might target the *Kl* gene (Predicted by bioinformatics software (http://www.targetscan.org/; http://www.microrna.org/microrna/microrna/home.do), these microRNAs were potentially targeting molecules that regulate Kl expression.). The results of qPCR showed that three of the ten potential microRNAs that targeted *Kl* expression (miR-15b, miR-497–5p, and miR-322) displayed a trend of increased expression in the ovarian tissue of POF mice. In particular, the increase in miR-15b expression was the most prominent (Fig. 5A). Similarly, the expression of miR-15b was significantly higher in mOGCs that had been isolated and cultured in vitro compared with the control (PBS-treated) group (Fig. 5B). Bioinformatics analysis revealed that two binding sites of miR-15b existed in the 3′ untranslated region (UTR) of the *Kl* mRNA, at 503-509bp and 1615-1622bp, respectively (Fig. 5C). The results of the luciferase reporter assays showed

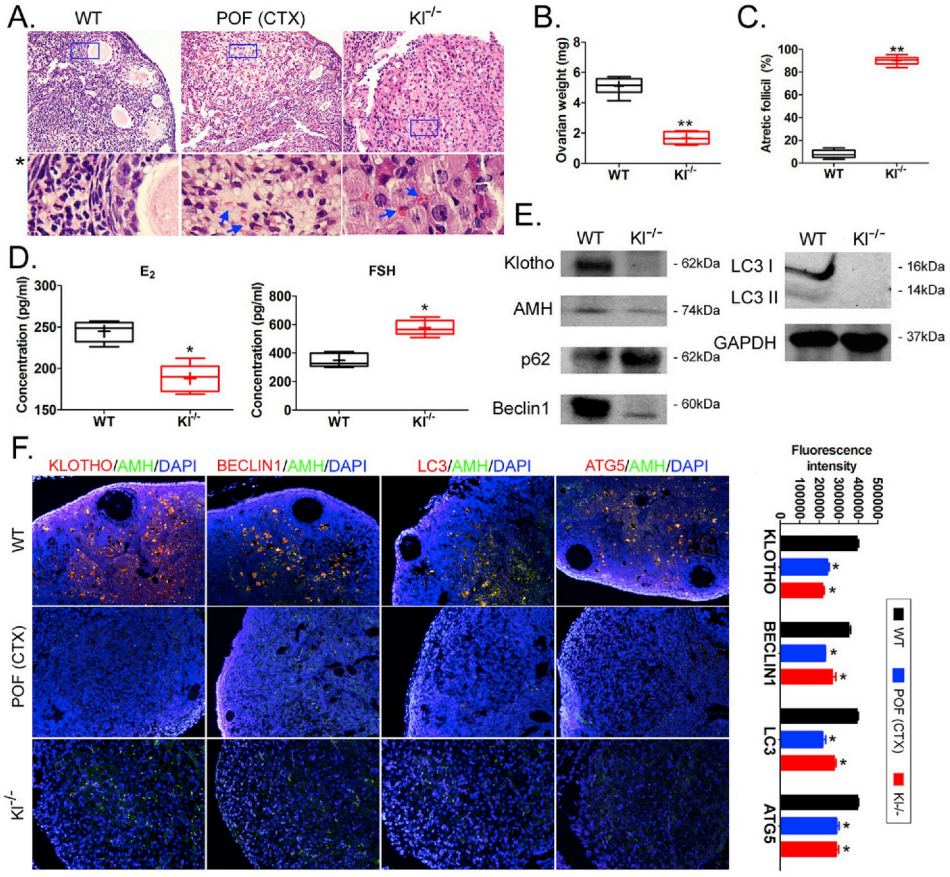

Fig. 3. Mice with homozygous knockout of *Kl* display a POF phenotype and a decrease in autophagy capacity. (A) H&E staining of ovarian tissues of the mice in each group. Magnification, 200 × . *Corresponds the magnified field of view outlined by the blue box. Magnification, 400 × . The blue arrows indicate areas of blood vessel rupture and bleeding. (B) Measurement of ovary weights in each group of mice. **p < 0.01 vs WT group; *t*-test; n = 6. (C) Determination of the proportion of atretic follicles in each group of mice. **p < 0.01 vs WT group; *t*-test; n = 6. (D) ELISA showing the hormone levels in the peripheral blood of mice in each group. *p < 0.05 vs WT group; *t*-test; n = 6. (E) Western blot showing the expression levels of Klotho and autophagy associated proteins in the ovarian tissues of each group of mice. (F) Immunofluorescence staining showing the expression levels of Klotho protein in the mOGCs (AMH+) in each group. Magnification, 200 × . *p < 0.05 vs WT group; *t*-test; n = 6. (For interpretation of the references to colour in this figure legend, the reader is referred to the Web version of this article.)

that miR-15b overexpression significantly suppressed the activity of the luciferase reporter harbouring the *Kl* 3′UTR (503-509bp), but it had minimal effect on the activity of the luciferase reporter harbouring the *Kl* 3′UTR (1615-1622bp) (Fig. 5D). The Western blot results showed that the expression of endogenous α-Klotho significantly decreased after the overexpression of miR-15b in mOGCs cultured in vitro, compared to it in overexpression of miR-mut in mOGCs (Fig. 5E, Supplement Data Fig. S2). These results indicated that miR-15b has the potential toreduce*Kl* expression.

In addition, CTX treatment on the miR-15b-overexpressing mOGCs (CTX-miR-15b-mOGCs) resulted in a significant increase in the inhibition rate of cell proliferation and apoptotic rate compared with CTX-miR-mut-mOGCs, PBS-miR-15b-mOGCs, and PBS-miR-mut-mOGCs (Fig. 5F, H). Meanwhile, the levels of α-Klotho and AMH protein expression in CTX-miR-15b-mOGCs were significantly lower than those in other groups (Fig. 5G, Supplement Data Fig. S2). These results suggested that the overexpression of miR-15b exacerbated the apoptosis of mOGCs.

Overexpression of miR-15b reduced the level of autophagy in mOGCs and attenuated their ROS scavenging and ATP synthesis ability.

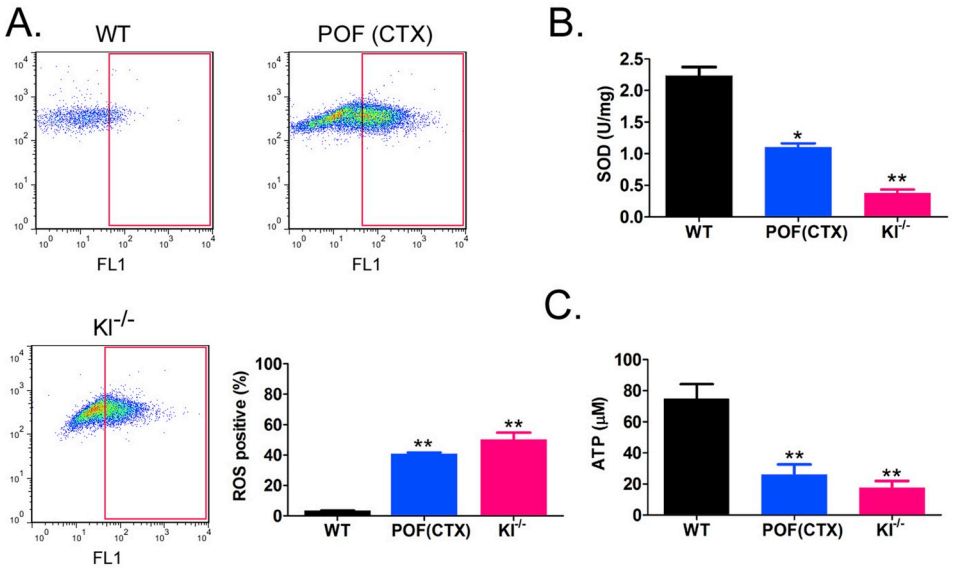

Fig. 4. Downregulation of *Kl* expression attenuates the ability of mOGCs to reduce oxidative stress. (A) Flow cytometry showing the proportions of ROS-positive mOGCs in each group of mice. **p < 0.01 vs WT group; *t*-test; n = 6. (B) SOD levels in the mOGCs of each group of mice. *p < 0.05 vs WT group; **p < 0.01 vs WT group; *t*-test; n = 6. (C) ATP levels in the mOGCs of each group of mice. **p < 0.01 vs WT group; *t*-test; n = 6.

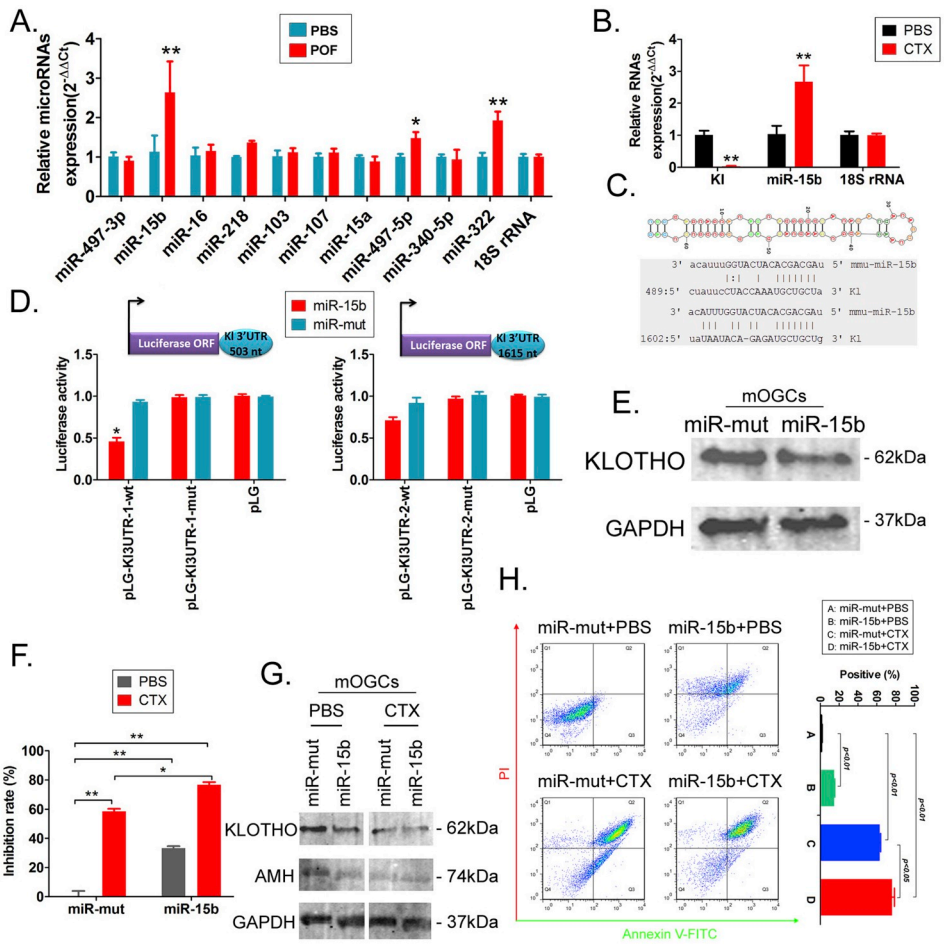

Fig. 5. CTX silences the expression of the endogenous target *Kl* via upregulating miR-15b expression. (A) qPCR showing the expression levels of multiple *Kl*-targeting microRNAs in the ovarian tissues of each group of mice. *p < 0.05 vs PBS group; **p < 0.01 vs PBS group; *t*-test; n = 6. (B) qPCR showing the expression levels of miR-15b in mOGCs treated with CTX or PBS. **p < 0.01 vs PBS group; *t*-test; n = 3. (C) Analysis of secondary structure of miR-15b and prediction of its target binding sites on the 3′UTR of *Kl* mRNA. (D) Luciferase reporter assay validation of the regulatory effects of miR-15b on the luciferase activities of reporters harbouring specific sites of the *Kl* mRNA 3′UTR. *p < 0.05 vs miR-mut group; *t*-test; n = 3. (E) Western blot showing the expression levels of Klotho protein in the mOGCs of each group of mice. (F) MTT assay showing the inhibition rates of cell proliferation in mOGCs transfected with miR-15b with or without CTX treatment. *p < 0.05; **p < 0.01; *t*-test; n = 3. (G) Western blot showing the expression levels of Klotho and AMH proteins in mOGCs transfected with miR-15b with or without CTX treatment. (H) Annexin V-FITC/PI staining and flow cytometry analysis on the apoptotic rates of mOGCs transfected with miR-15b with or without CTX treatment. *t*-test; n = 3.

Western blot analysis showed that the expression levels of the autophagy-related proteins Beclin 1 and LC3I/II were considerably lower in the miR-15b-overexpressing mOGCs than in the control group (miR-mut-mOGCs) (Fig. 6A, Supplement Data Fig. S2). And, immunofluorescence staining revealed that in miR-15b-overexpressing mOGCs, not only were the signals for AMH and α-Klotho expression significantly attenuated, but the signals for autophagy-related proteins were as well (Fig. 6B). Meanwhile, transmission electron microscopy also showed that there was a significant reduction in the number of mitochondria, poorer structural integrity, and a significant decrease in the number of autophagosomes in miR-15b-mOGCs (Fig. 6C). These results suggested that overexpression of miR-15b induced a reduction in the level of autophagy in mOGCs.

Furthermore, the ROS assay showed that the ROS level was higher in the miR-15b-overexpressing mOGCs than in the control group of miR-mut-overexpressing mOGCs (Fig. 7A). However, the SOD level was significantly lower in miR-15b-mOGCs than in the miR-mut group (Fig. 7B). Meanwhile, the ATP level was also lower in miR-15b-mOGCs than in the control group (Fig. 7C). These results suggested that the overexpression of miR-15b significantly attenuated the ROS scavenging and ATP synthesis ability of mOGCs.

3.4. Suppression of Klexpression affected the expression of the TGF-β/Smadpathway in mOGCs

As the TGF-β/Smad pathway is closely related to ageing, fibrosis, and autophagy, we examined the expression of the TGF-β/Smad pathway in each group of cells. First, qPCR results showed that in the ovaries of $Kl^{-/-}$ mice with CTX-induced POF, the expression of the respective signalling molecule of the TGF-β/Smad pathway was significantly higher than that in the WT mice, whereas the mRNA expression of autophagy-related molecules was reduced (Fig. 8A). Meanwhile, the expression of the respective signalling molecule of the TGF-β/Smad pathway was significantly higher in the miR-15b-overexpressing mOGCs than in the control group, whereas the mRNA expression of autophagy-related molecules was reduced (Fig. 8B). The Western blot results also indicated that the expression levels of the TGF-β/Smad pathway signalling molecules, including the protein levels of TGF-β1, Smad2, and Smad3, and the phosphorylation levels of *p*-Smad2 and *p*-Smad3, were significantly higher in the ovaries of both the $Kl^{-/-}$ mice with CTX-induced POF and in the miR-15b-overexpressing mOGCs than in the control groups (Fig. 8C, Supplement Data Fig. S2). These results indicated that the suppression of *Kl* expression significantly upregulated the expression of the TGF-β/Smad pathway.

4. Discussion

POF is a typical gynaecological disease that has a significant impact on the reproductive health of women and is one of the root causes of infertility [3,8,11,13]. The pathogenesis of POF is complex and can be affected by many factors [3,8,11,13]. Our previous studies have focused on the investigations of POF induced by aberrant epigenetic modifications [1–4,8–11,13]. These previous studies have found that the aberrant expression of certain microRNAs and long non-coding RNAs in the mouse model of POF induced by either CTX or tripterygium glycosides can result in damage to and ageing of mOGCs, leading to the development of POF [2,8,11,13]. Moreover, we have also found that the development of POF is accompanied by the pathological ageing of mOGCs [11,13]. Therefore, we hypothesised that the development of POF was a type of pathological ageing. Our observation of ageing in mOGCs had naturally led us to study

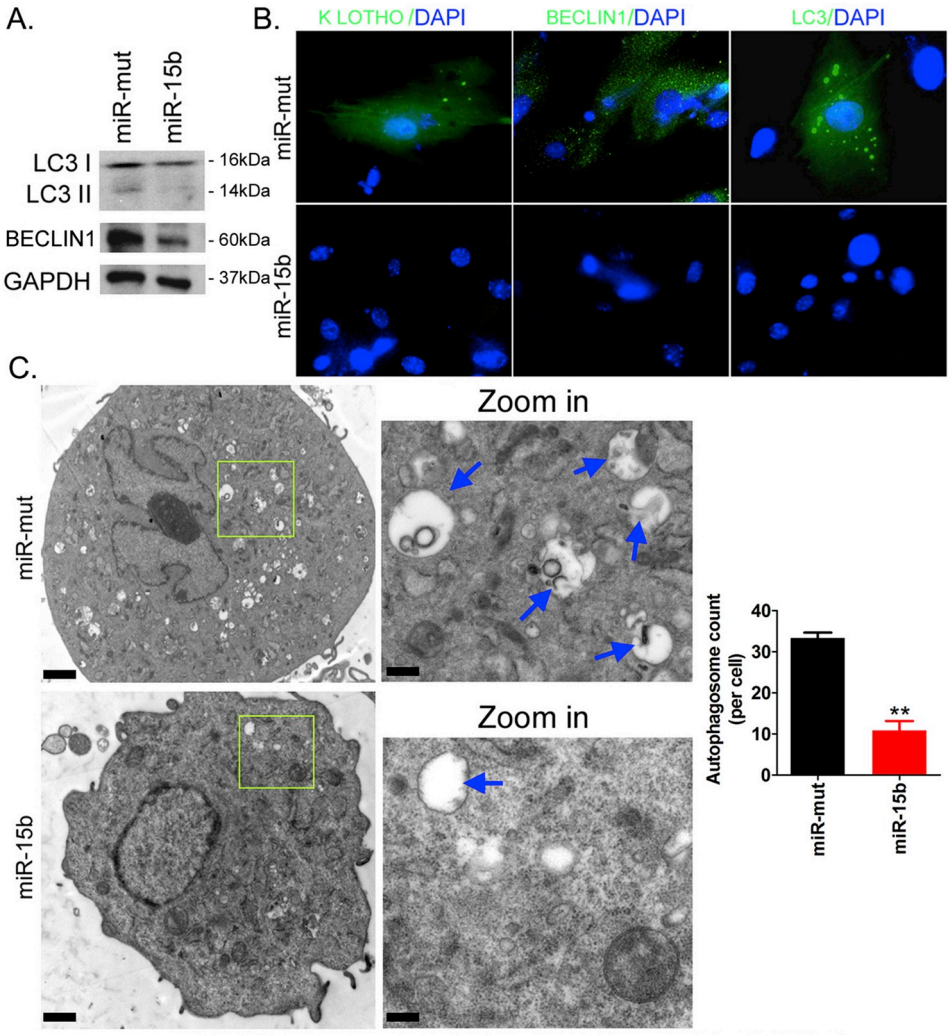

Fig. 6. Overexpression of miR-15b inhibits autophagy activity in mOGCs. (A) Western blot analysis showing the expression levels of endogenous autophagy-related proteins in mOGCs transfected with miR-15b. (B) Immunofluorescence staining showing the expression levels of endogenous autophagy-related proteins in the mOGCs of each group of mice. Magnification, 200 × . (C) Transmission electron microscopy analysis of the autophagosomal structures in the mOGCs of each group of mice. Scale bar = 2.0 μm **p < 0.01 vs miR-mut transfection group.

the Klotho gene. In recent years, there has been an increasing number of studies concerning the differential expression of the Klotho protein and its effects on ageing and fibrosis in various organs [16–18,21–23,25,29,30]. Many studies have demonstrated that the artificial reduction in Klotho protein expression causes not only liver and kidney fibrosis, but also the ageing of many organs [16–18,21–23,25,29,30]. As early as 1997, studies have shown that genetically manipulated mice deficient in α-Klotho or fibroblast growth factor 23 (FGF23) exhibited premature ageing, including early onset of cardiovascular disease, cancer, and cognitive decline [16–18,21–23,25,29,30]. Studies on structural biology have suggested that α-Klotho functions as a subunit that assists FGF23 in controlling lifespan [16,18,27]. Based on the above findings, we first examined the expression of Klotho in the ovarian tissue of a mouse model with CTX-induced POF. The study results were consistent with our hypothesis that CTX intervention in mice could significantly reduce Klotho expression in mOGCs. Then we examinedwhether knockout of Klotho in normal WT mice would also lead to POF. We conducted detailed investigations on the reproductive system and hormone levels of female mice with homozygous Klotho knockout ($Kl^{-/-}$). The results demonstrated that the weight of ovarian tissue was significantly reduced in $Kl^{-/-}$ mice. The mOGCs lost the morphology as interstitial cells. The number of atretic follicles in the ovary was significantly increased, whereas the number of normal follicles was reduced. Additionally, FSH concentration was significantly increased, whereas the E2 concentration in the peripheral blood of $Kl^{-/-}$ mice wasreduced. All results in this study showed that $Kl^{-/-}$ mice exhibited significant follicular atresia and ovarian insufficiency, and their phenotypes were highly similar to that of POF. In addition, we selected *C. elegans* as another biological model to validate our hypothesis in a different organism. *C. elegans* was chosen because they harbour two genes, C50F7.10 and E02H9.5 (ceKlotho), which are highly homologous to the α-Klotho gene in mammals. We found that CTX intervention could significantly inhibit various normal physiological behaviours in *C. elegans*, and it could shorten their lifespan. At the same time, CTX could reduce the ovulation rate and fertility of *C. elegans*. These abnormal conditions observed in *C. elegans* were due to the inhibition of both the endogenous ceKlotho and the IIS longevity signalling pathway by CTX. Therefore, we have demonstrated that the loss of *Kl* can lead to pathological ageing and reduced oestrogen release in the reproductive system of female mice, resulting in a significant decrease in their fertility [1–4,8–11,13,16–18,21–23,25,27,29,30].

Previous reports have shown that the internal autophagy process is specifically regulated by Klotho during stem cell differentiation into mature adipocytes [30], and that α-Klotho mitigates the progression of acute kidney injury (AKI) to chronic kidney disease (CKD) through activation of autophagy [31]. Many studies have also reported that an imbalance in autophagy is closely associated with abnormal ageing of body organs. Therefore, we directed our focus onto the internal link

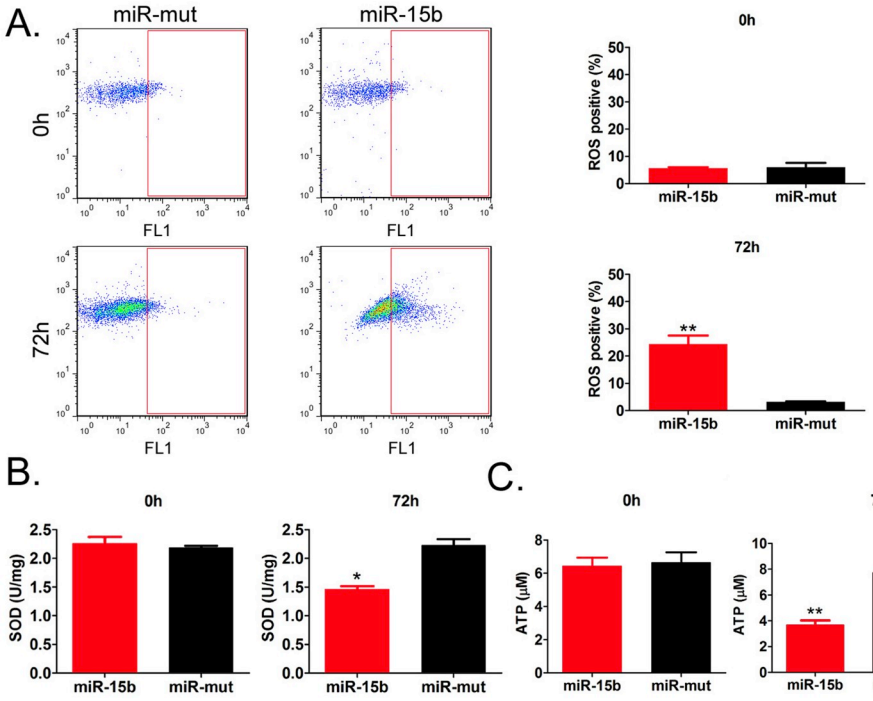

Fig. 7. Overexpression of miR-15b attenuates the ability of mOGCs to reduce oxidative stress. (A) Flow cytometry showing the proportions of ROS-positive mOGCs in each group of mice. **p < 0.01 vs miR-mut transfection group; *t*-test; n = 3. (B) SOD levels in the mOGCs of each group of mice. *p < 0.05 vs miR-mut transfection group; *t*-test; n = 3. (C) ATP levels in the mOGCs of each group of mice. **p < 0.01 vs miR-mut transfection group; *t*-test; n = 3.

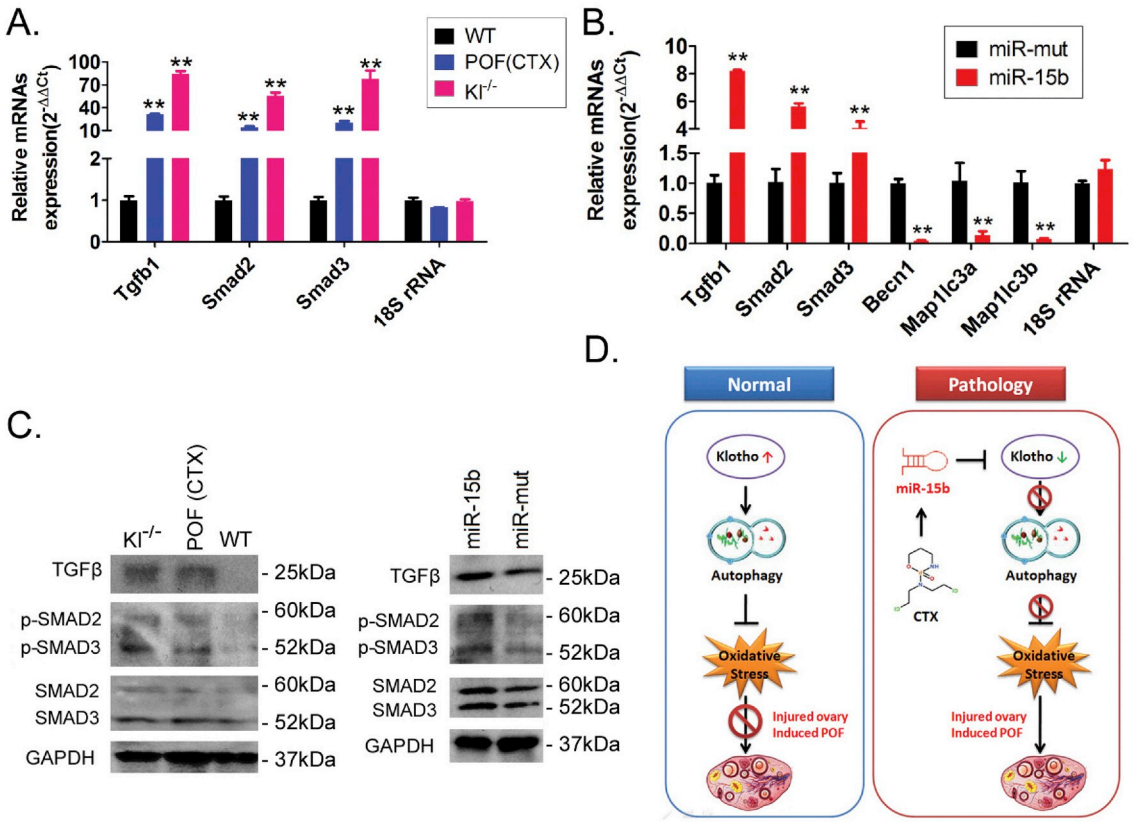

Fig. 8. Downregulation of *Kl* expression activates the TGF-β/Smad signalling pathway in the ovaries of mice. (A) qPCR showing the mRNA expression levels of key factors of the TGF-β/Smad signalling pathway in the ovarian tissues of each group of mice. **p < 0.01 vs WT group; *t*-test; n = 6. (B) qPCR showing the mRNA expression levels of key factors of the TGF-β/Smad signalling pathway in the mOGCs of each group. **p < 0.01 vs miR-mut transfection group; *t*-test; n = 3. (C) Western blot showing the expression levels of key proteins of the TGF-β/Smad signalling pathway in the ovarian tissues of each group of mice. (D) Western blot showing the expression levels of key proteins of the TGF-β/Smad signalling pathway in the mOGCs of each group of mice. (E) The mechanism of inducing POF by CTX-dependent miR-15b via the suppression of α-Klotho expression in mOGCs.

between autophagy and POF in this study. We found that both the CTX-induced POF mouse model and $Kl^{-/-}$ mice had a significant reduction in the autophagy-related factors such as LC3 and Beclin1 in their mOGCs, which was suggestive of abnormal autophagic behaviour. Meanwhile, the endogenous TGF-β/Smad signalling transduction pathway was also activated after the downregulation of *Kl* expression. Further investigations confirmed that mOGCs exhibited oxidative stress when the level of autophagy was significantly reduced along with decreased SOD activity, increased ROS level, and decreased amount of ATP. These results reflect the reduced ability of the body to scavenge ROS and the increased extent of ageing in organelles [30,31].

We demonstrated through a series of experiments that the development of ovarian insufficiency and POF caused by decreased *Kl* expression is largely due to the dysfunction or reduced capacity of autophagy function in mOGCs, which reduces its ROS scavenging ability. Excessive ROS damages the organelles and results in a decrease in the amount of ATP, which leads to an insufficient supply to the cells. As the cells are unable to perform normal physiological and biochemical activities, this ultimately limits the function of the mOGCs. However, the final question that still needed to be understood was what caused the reduced expression of endogenous Klotho in the ovaries of CTX-treated mice. Since our previous research on POF pathogenesis had mainly focused on the levels of non-coding RNAs, we directed our attention to the regulatory effects of microRNAs in this study [11,13]. Upon screening, we found that the α-Klotho gene was a potential target of miR-15b, and the expression level of miR-15b in the mOGCs of CTX-stimulated mice was significantly elevated. This indicated that the expression of miR-15b was positively induced by CTX. We subsequently overexpressed miR-15b in mOGCs and found that, compared with the control group, these cells exhibited a phenotype with autophagy dysfunction, elevated levels of ROS, and abnormal energy metabolism. Moreover, we also found that the overexpression of miR-15b in mOGCs not only significantly reduced the expression of endogenous Klotho, but also reduced the expression of autophagy-related factors and promoted the elevated expression of signalling molecules of the TGF-β/Smad pathway.

Therefore, our study demonstrated that the loss of Klotho expression activated the downstream TGF-β/Smad signalling pathway, resulting in decreased autophagy activity. This reduced the ability of the cells to scavenge ROS, ultimately hampering normal cellular function and inducing apoptosis.

Author disclosure statement

We declared no potential conflicts of interest.

Acknowledgements

This work was supported by grant from Shanghai Natural Science Foundation (No. 16ZR1434000). And, grant from the projects sponsored by the development fund for Shanghai talents (2017054). And, grant from the projects sponsored by the fund for Xinglin talents of Shanghai University of TCM (201707081). And, grant from the graduate student innovation training project of Shanghai University of Traditional Chinese Medicine (Y201860). We declared no potential conflicts of interest.

Appendix A. Supplementary data

Supplementary data to this article can be found online at https://doi.org/10.1016/j.freeradbiomed.2019.07.010.

References

[1] T. Liu, Y. Huang, L. Guo, W. Cheng, G. Zou, CD44+/CD105+ human amniotic fluid mesenchymal stem cells survive and proliferate in the ovary long-term in a mouse model of chemotherapy-induced premature ovarian failure, Int. J. Med. Sci. 9 (7) (2012) 592–602.

[2] T. Liu, W. Qin, Y. Huang, Y. Zhao, J. Wang, Induction of estrogen-sensitive epithelial cells derived from human-induced pluripotent stem cells to repair ovarian function in a chemotherapy-induced mouse model of premature ovarian failure, DNA Cell Biol. 32 (12) (2013) 685–698.

[3] T. Liu, Y. Huang, J. Zhang, W. Qin, H. Chi, J. Chen, Z. Yu, C. Chen, Transplantation of human menstrual blood stem cells to treat premature ovarian failure in mouse model, Stem Cells Dev. 23 (13) (2014) 1548–1557.

[4] T.E. Liu, L. Zhang, S. Wang, C. Chen, J. Zheng, Tripterygium glycosides induce premature ovarian failure in rats by promoting p53 phosphorylation and activating the serine/threonine kinase 11-p53-p21 signaling pathway, Exper. Therapeut. Med. 10 (1) (2015) 12–18.

[5] W. Pan, X. Ye, S. Yin, X. Ma, C. Li, J. Zhou, W. Liu, J. Liu, Selected persistent organic pollutants associated with the risk of primary ovarian insufficiency in women, Environ. Int. 129 (2019) 51–58.

[6] G. Yao, J. He, Y. Kong, J. Zhai, Y. Xu, G. Yang, D. Kong, F. Dong, S. Shi, Q. Yang, Y. Sun, Transcriptional profiling of long noncoding RNAs and their target transcripts in ovarian cortical tissues from women with normal menstrual cycles and primary ovarian insufficiency, Mol. Reprod. Dev. (2019), https://doi.org/10.1002/mrd.23158.

[7] J.P. Christ, M.N. Gunning, G. Palla, M.J.C. Eijkemans, C.B. Lambalk, J.S.E. Laven, B. Fauser, Estrogen deprivation and cardiovascular disease risk in primary ovarian insufficiency, Fertil. Steril. 109 (4) (2018) 594–600 e1.

[8] T. Liu, S. Wang, Q. Li, Y. Huang, C. Chen, J. Zheng, Telocytes as potential targets in a cyclophosphamide-induced animal model of premature ovarian failure, Mol. Med. Rep. 14 (3) (2016) 2415–2422.

[9] T.E. Liu, S. Wang, L. Zhang, L. Guo, Z. Yu, C. Chen, J. Zheng, Growth hormone treatment of premature ovarian failure in a mouse model via stimulation of the Notch-1 signaling pathway, Exper. Therapeut. Med. 12 (1) (2016) 215–221.

[10] T. Liu, Q. Li, S. Wang, C. Chen, J. Zheng, Transplantation of ovarian granulosalike cells derived from human induced pluripotent stem cells for the treatment of murine premature ovarian failure, Mol. Med. Rep. 13 (6) (2016) 5053–5058.

[11] Y. Xiong, T. Liu, S. Wang, H. Chi, C. Chen, J. Zheng, Cyclophosphamide promotes the proliferation inhibition of mouse ovarian granulosa cells and premature ovarian failure by activating the lncRNA-Meg3-p53-p66Shc pathway, Gene 596 (2017) 1–8.

[12] P. Laissue, The molecular complexity of primary ovarian insufficiency aetiology and the use of massively parallel sequencing, Mol. Cell. Endocrinol. 460 (2018) 170–180.

[13] A. Ai, Y. Xiong, B. Wu, J. Lin, Y. Huang, Y. Cao, T. Liu, Induction of miR-15a expression by tripterygium glycosides caused premature ovarian failure by suppressing the Hippo-YAP/TAZ signaling effector Lats1, Gene 678 (2018) 155–163.

[14] M. Kuro-o, Y. Matsumura, H. Aizawa, H. Kawaguchi, T. Suga, T. Utsugi, Y. Ohyama, M. Kurabayashi, T. Kaname, E. Kume, H. Iwasaki, A. Iida, T. Shiraki-Iida, S. Nishikawa, R. Nagai, Y.I. Nabeshima, Mutation of the mouse klotho gene leads to a syndrome resembling ageing, Nature 390 (6655) (1997) 45–51.

[15] I. Urakawa, Y. Yamazaki, T. Shimada, K. Iijima, H. Hasegawa, K. Okawa, T. Fujita, S. Fukumoto, T. Yamashita, Klotho converts canonical FGF receptor into a specific receptor for FGF23, Nature 444 (7120) (2006) 770–774.

[16] Y. Xu, Z. Sun, Molecular basis of Klotho: from gene to function in aging, Endocr. Rev. 36 (2) (2015) 174–193.

[17] A. Bian, J.A. Neyra, M. Zhan, M.C. Hu, Klotho, stem cells, and aging, Clin. Interv. Aging 10 (2015) 1233–1243.

[18] G. Chen, Y. Liu, R. Goetz, L. Fu, S. Jayaraman, M.C. Hu, O.W. Moe, G. Liang, X. Li, M. Mohammadi, alpha-Klotho is a non-enzymatic molecular scaffold for FGF23 hormone signalling, Nature 553 (7689) (2018) 461–466.

[19] E.S. Kuzina, P.M. Ung, J. Mohanty, F. Tome, J. Choi, E. Pardon, J. Steyaert, I. Lax, A. Schlessinger, J. Schlessinger, S. Lee, Structures of ligand-occupied beta-Klotho complexes reveal a molecular mechanism underlying endocrine FGF specificity and activity, Proc. Natl. Acad. Sci. U. S. A. 116 (16) (2019) 7819–7824.

[20] O.M. Kuro, The Klotho proteins in health and disease, Nat. Rev. Nephrol. 15 (1) (2019) 27–44.

[21] A. Gazdhar, P. Ravikumar, J. Pastor, M. Heller, J. Ye, J. Zhang, O.W. Moe, T. Geiser, C.C.W. Hsia, Alpha-Klotho enrichment in induced pluripotent stem cell secretome contributes to antioxidative protection in acute lung injury, Stem Cells 36 (4) (2018) 616–625.

[22] Y. Qian, X. Guo, L. Che, X. Guan, B. Wu, R. Lu, M. Zhu, H. Pang, Y. Yan, Z. Ni, L. Gu, Klotho reduces necroptosis by targeting oxidative stress involved in renal ischemic-reperfusion injury, cellular physiology and biochemistry, Int. J. Exper. Cell. Physiol. Biochem. Pharmacol. 45 (6) (2018) 2268–2282.

[23] T. Kimura, K. Shiizaki, H. Kurosu, T. Akimoto, T. Shinzato, T. Shimizu, A. Kurosawa, T. Kubo, K. Nanmoku, O.M. Kuro, T. Yagisawa, The impact of preserved Klotho gene expression on anti-oxidative stress activity in healthy kidney, Am. J. Physiol. Renal Physiol. 315 (2) (2018) F345–F352, https://doi.org/10.1152/ajprenal.00486.2017.

[24] K. Chen, Z. Sun, Activation of DNA demethylases attenuates aging-associated arterial stiffening and hypertension, Aging Cell (2018) e12762.

[25] T. Minamizaki, Y. Konishi, K. Sakurai, H. Yoshioka, J.E. Aubin, K. Kozai, Y. Yoshiko, Soluble Klotho causes hypomineralization in Klotho-deficient mice, J. Endocrinol. 237 (3) (2018) 285–300.

[26] P. Chuchana, A.L. Mausset-Bonnefont, M. Mathieu, F. Espinoza, M. Teigell, K. Toupet, C. Ripoll, F. Djouad, D. Noel, C. Jorgensen, J.M. Brondello, Secreted alpha-Klotho maintains cartilage tissue homeostasis by repressing NOS2 and ZIP8-MMP13 catabolic axis, Aging 10 (6) (2018) 1442–1453.

[27] S. Lee, J. Choi, J. Mohanty, L.P. Sousa, F. Tome, E. Pardon, J. Steyaert, M.A. Lemmon, I. Lax, J. Schlessinger, Structures of beta-klotho reveal a 'zip code'-

like mechanism for endocrine FGF signalling, Nature 553 (7689) (2018) 501–505.
[28] S. Sato, Y. Kawamata, A. Takahashi, Y. Imai, A. Hanyu, A. Okuma, M. Takasugi, K. Yamakoshi, H. Sorimachi, H. Kanda, Y. Ishikawa, S. Sone, Y. Nishioka, N. Ohtani, E. Hara, Ablation of the p16(INK4a) tumour suppressor reverses ageing phenotypes of klotho mice, Nat. Commun. 6 (2015) 7035.
[29] R.H. Iida, S. Kanko, T. Suga, M. Morito, A. Yamane, Autophagic-lysosomal pathway functions in the masseter and tongue muscles in the klotho mouse, a mouse model for aging, Mol. Cell. Biochem. 348 (1–2) (2011) 89–98.
[30] J. Fan, Z. Sun, The antiaging gene klotho regulates proliferation and differentiation of adipose-derived stem cells, Stem Cells 34 (6) (2016) 1615–1625.
[31] M. Shi, B. Flores, N. Gillings, A. Bian, H.J. Cho, S. Yan, Y. Liu, B. Levine, O.W. Moe, M.C. Hu, alphaKlotho mitigates progression of AKI to CKD through activation of autophagy, J. Am. Soc. Nephrol. 27 (8) (2016) 2331–2345.
[32] F. Solari, CeKlotho opens a new road for investigation in worm aging, Aging 2 (9) (2010) 539–540.
[33] Y. Seo, S. Kingsley, G. Walker, M.A. Mondoux, H.A. Tissenbaum, Metabolic shift from glycogen to trehalose promotes lifespan and healthspan in Caenorhabditis elegans, Proc. Natl. Acad. Sci. U. S. A. 115 (12) (2018) E2791–E2800.
[34] U.M. Polanska, E. Edwards, D.G. Fernig, T.K. Kinnunen, The cooperation of FGF receptor and Klotho is involved in excretory canal development and regulation of metabolic homeostasis in Caenorhabditis elegans, J. Biol. Chem. 286 (7) (2011) 5657–5666.
[35] R. Kaletsky, C.T. Murphy, The role of insulin/IGF-like signaling in C. elegans longevity and aging, Dis. Model Mech. 3 (7–8) (2010) 415–419.
[36] M.T. Chateau, C. Araiz, S. Descamps, S. Galas, Klotho interferes with a novel FGF-signalling pathway and insulin/Igf-like signalling to improve longevity and stress resistance in Caenorhabditis elegans, Aging 2 (9) (2010) 567–581.